# Conductive and anti-freezing hydrogels constructed by pseudo-slide-ring networks

| | |
|---|---|
| Journal: | *ChemComm* |
| Manuscript ID | CC-COM-09-2021-005527.R1 |
| Article Type: | Communication |
| | |

COMMUNICATION

# Conductive and anti-freezing hydrogels constructed by pseudo-slide-ring networks

Qianming Lin [a] and Chenfeng Ke*[a]

Received 00th January 20xx,
Accepted 00th January 20xx

DOI: 10.1039/x0xx00000x

**Stretchable, tough, and anti-freezing hydrogels were prepared using partially carboxymethylated polyrotaxanes and polyacrylamides. The carboxylic acid groups of α-cyclodextrins in the polyrotaxane and the amide groups in polyacrylamide are hydrogen-bonded, affording a pseudo-slide-ring network, greatly enhancing the hydrogels' macroscale mechanical properties, anti-freezing features, and electrical conductivity for the fabrication of a cold-temperature strain sensor.**

Hydrogels have been extensively investigated for applications in diagnostics,[1,2] drug delivery,[3,4] implants,[5,6] and wearable devices.[7,8] At sub-zero temperatures, the freezing of water molecules within hydrogels causes structural failure and functional loss. Maintaining hydrogels' flexibility and mechanical robustness below 0 °C is critical for use in extreme environments such as cold regions[9] or missions in outer space.[10] To date, the introduction of inorganic salts,[11] organic solvents,[12] ionic liquids (ionogels)[13] have been successfully demonstrated in lowering the freezing point of hydrogels. However, these additives can easily leak into the environment and possibly compromise their mechanical properties.[14] In contrast, developing polymeric materials[15] with designed molecular entities[16] and network architectures[17] to suppress ice formation and growth is promising for the development of anti-freezing hydrogels with good mechanical properties.

An effective strategy to retard the nucleation and growth of ice crystals[18] in a hydrogel is introducing hydrogen-bonding moieties.[19] These building blocks bind water[20] and segregate ice clusters/crystals in hydrophobic[21] or hydrophilic networks.[22] For example, grafting hydrophobic alkyl side chains[23] to a polymer backbone and polyethylene glycol (PEG)[19] reduced the water freezing point to –8 °C and –20 °C, respectively. In these cases, the high grafting density of the anti-freezing groups often shows a negative impact on the mechanical performance of the hydrogel.[14] To achieve a balance between good anti-freezing capabilities and high mechanical strength and elasticity, in this work, we introduced a pseudo-slide-ring hydrogel consisting of a polyrotaxane-based hydrogen-bonding crosslinker (Fig. 1) and polyacrylamide, which simultaneously demonstrates a low freezing point (－25 °C), high stretchability (740%), high toughness (1100 kJ/m$^3$), and high strength (tensile stress 156 kPa). Furthermore, this pseudo-slide-ring hydrogel is also conductive, which enabled us to fabricate a strain sensor that functions at cold temperatures.

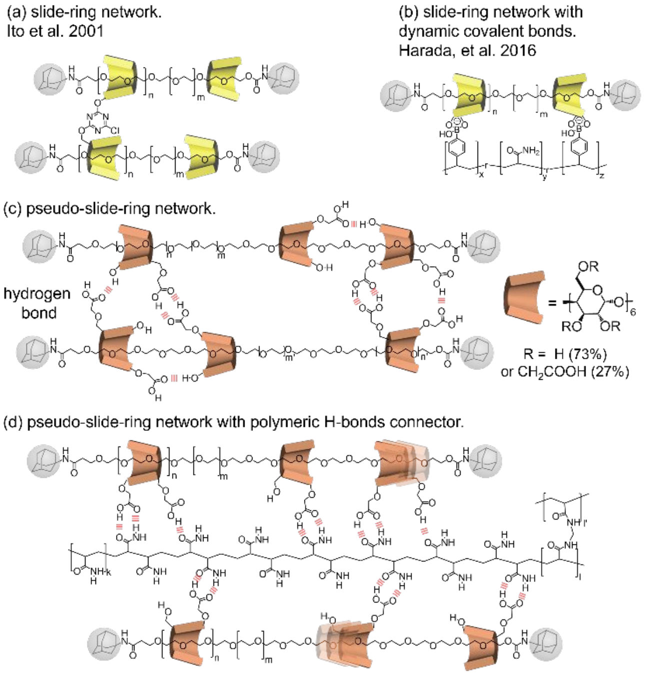

**Fig 1**. Graphical representations of (a) a slide-ring network,[23] (b) a slide-ring network connected through dynamic covalent bonds,[28] and (c-d) pseudo-slide-ring networks connected via hydrogen-bonding interactions.

The slide-ring network, coined by Ito et al.,[24,25] is comprised of mobile crosslinkers (cyclodextrin dimers) and polyethylene

---

[a] Department of Chemistry, Dartmouth College, 41 College Street, Hanover, NH 03755, USA. Email: chenfeng.ke@dartmouth.edu

Electronic Supplementary Information (ESI) available: [details of any supplementary information available should be included here]. See DOI: 10.1039/x0xx00000x

glycol axles (Fig. 1a). The mobile α-cyclodextrin (α-CD) crosslinkers can translocate along the PEG axles when the material is stretched[26] or compressed.[27] During these processes, the crosslinking points of the network moved to increase the toughness and stretchability of the hydrogels.[28] Instead of using covalent linkages to bridge CDs, Harada et al.[29] introduced dynamic boronic esters to form CD crosslinkers (Fig. 1b), adding a self-healing property to the slide-ring hydrogel. Further reducing the bond strength between the mobile CD crosslinkers to non-covalent interactions, such as hydrogen-bonding in carboxylic acid dimers, form a pseudo-slide-ring (PSR) network (Fig. 1c). In an ideal PSR network, carboxylic acid modified α-CDs are hydrogen-bonded[30] ($\Delta G = -7.1$ kcal/mol) as mobile crosslinkers, which can translocate along the PEG axle rapidly at room temperature (energy barrier $E_a = 2.1$ kcal/mol).[31] The introduced carboxylic moieties can bind water to enhance the anti-freezing properties of the hydrogel. When ice crystals are formed at sub-zero temperatures, the mechanical stress caused by the water-to-ice volume expansion will be dissipated by the PSR network, which is expected to decelerate the ice crystal growth rate.[17]

Partially carboxylic acid-substituted polyrotaxane $PR_{COOH}$ was selected as the candidate for the construction of the PSR network. $PR_{COOH}$ was synthesized using PEG-$(CO_2H)_2$ ($M_n = 35$ kDa) and α-CD following a previously reported method.[32] Briefly, a native α-CD-based polyrotaxane was synthesized[33] with ~107 α-CDs capped by the adamantyl (Ad) end groups on the PEG axle (Fig. S5). Carboxymethylation of this polyrotaxane afforded $PR_{COOH}$ with an averaged 27 ± 2% substitution degree (4.9 ± 0.3 carboxymethyl groups on each α-CD, Fig. S6-8). When the concentration of $PR_{COOH}$ reached 1.2 mM (20 wt%, [COOH] = 0.62 M, Table S1), a stable hydrogel was formed at pH 4, suggesting the formation of a stable hydrogen-bonded network (Fig. 2a and S14). At low strain (0.1%), the elastic moduli (G′) of hydrogel remained constant at all tested frequencies, indicating α-CDs had very limited mobility along the PEG axle, which could be attributed to the α-CD-α-CD aggregation along the PEG axle and between neighboring $PR_{COOH}$ via the hydrogen-bonding interactions between the carboxylic groups (COOH) and residual hydroxyl groups (OH).

To inhibit the undesired COOH•••OH hydrogen-bonding interactions between the carboxymethylated α-CDs, an excess of polyacrylamide (PAAm, $M_n = 10$ kDa) was introduced to establish amide-carboxylic acid (Am•••COOH) hydrogen-bonding interaction ($\Delta G = -8.6$ kcal/mol).[30] PAAm also serves as a polymeric hydrogen-bonding mediator (Fig. 1d) to generate an effective PSR network. Gradually increasing the amount of PAAm to $PR_{COOH}$ resulted in the elastic moduli (G′) of the hydrogel decreasing, and G′ became frequency-dependent (Fig. 2a). When [Am]/[COOH] reached 18:1, the hydrogel was converted to a viscous liquid (Fig. S16 and 17), showing strong frequency-dependent elastic moduli. $^1$H NMR investigations (Fig. 13-14) showed that the carboxymethyl groups and α-CDs are in close proximity to the backbone of PAAm. These results suggested the successful disruption of the undesired carboxymethylated α-CD aggregations. The viscosity of the sample gradually increased when non-viscous PAAm was added to the solution of $PR_{COOH}$ (blue, Fig. 2b and S16), suggesting the formation of multivalent hydrogen-bonding interactions between amide and COOH groups. When [Am]:[COOH] ratio reached 18:1, the PSR was nearly a Newtonian fluid (Fig. 2b), suggesting that the PSR network possesses minimum entangled structures[34] and high PAAm-loaded PSR allows for fast hydrogen-bonding site exchanging upon shearing.

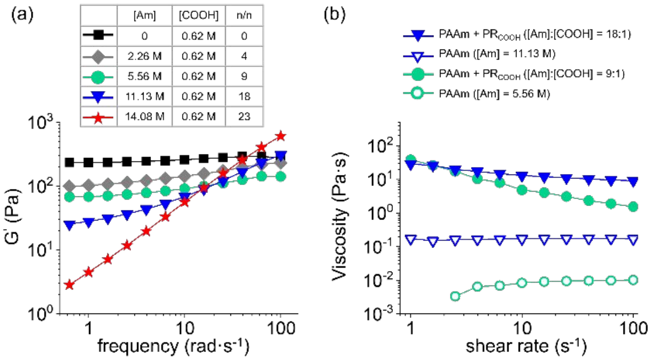

**Fig 2**. (a) Frequency-dependent elastic moduli G′ and (b) viscosities of the samples formed by $PR_{COOH}$ (20 wt%, 0.62 M of COOH) and different amounts of linear PAAm (0, 2.46, 5.56, 11.13, 14.08 M of Am). The molar ratios of [Am]/[COOH] changed from 0 to 23:1. The viscosities of PAAm solutions were provided as references.

PAAm/$PR_{COOH}$ PSR hydrogels were synthesized by polymerizing acrylamide monomer (2.8 M, 20 w/v%), *N,N′*-methylenebisacrylamide crosslinker (0.84% equivalent to acrylamide) in the presence of different amounts of $PR_{COOH}$ (2, 5, and 10 wt%, 0.05, 0.13, and 0.26 M of COOH, respectively) in aqueous solutions (pH 4). Ammonium persulfate ($(NH_4)_2S_2O_8$, 22 mM) and tetramethylethylenediamine (67 mM) were used as the initiator and catalyst, respectively.[11] The photo-polymerizations were carried out at room temperature overnight in a rectangular Teflon$^{TM}$ mold (40 × 8 × 2 mm, Fig. S14). The crosslinked PSR hydrogels are named as $PSR_{2wt}$, $PSR_{5wt}$, and $PSR_{10wt}$, respectively (see ESI for details).

The mechanical properties of the PSR hydrogels were investigated through tensile tests. In the absence of $PR_{COOH}$, the crosslinked PAAm hydrogel showed limited Young's modulus and stretchability (blue, Fig. 3a). In the presence of 2 wt% of $PR_{COOH}$, the $PSR_{2wt}$ hydrogel ([Am]/[COOH] = 46:1) demonstrated improved stretchability (400 %, black, Fig. 3a). Increasing the $PR_{COOH}$ to 5 wt%, the $PSR_{5wt}$ hydrogel ([Am]/[COOH] = 18:1) was stretched up to 740 % with a measured toughness of 1100 kJ/m$^3$. $PSR_{5wt}$ is 3 times more stretchable and 30 times tougher than PAAm hydrogel (red, Fig. 3a). Further increasing the $PR_{COOH}$ to 10 wt%([Am]/[COOH] = 9:1), the hydrogel turned brittle and its Young's modulus reached 300 kPa. From $PSR_{2wt}$ to $PSR_{10wt}$ hydrogels, the ratios between the [Am]/[COOH] changed from 46:1 to 9:1. While the Young's moduli of the hydrogels were enhanced with the increased population of hydrogen-bonding pairs, the stretchability of the hydrogels reached an optimum value at the [Am]/[COOH] ratio of 18 (5 wt% $PR_{COOH}$). The concentrated carboxymethylated CDs are well-spaced due to the excess of PAAm chains in the optimal PSR network, where the COOH•••$NH_2$ hydrogen-bonding interactions allow the

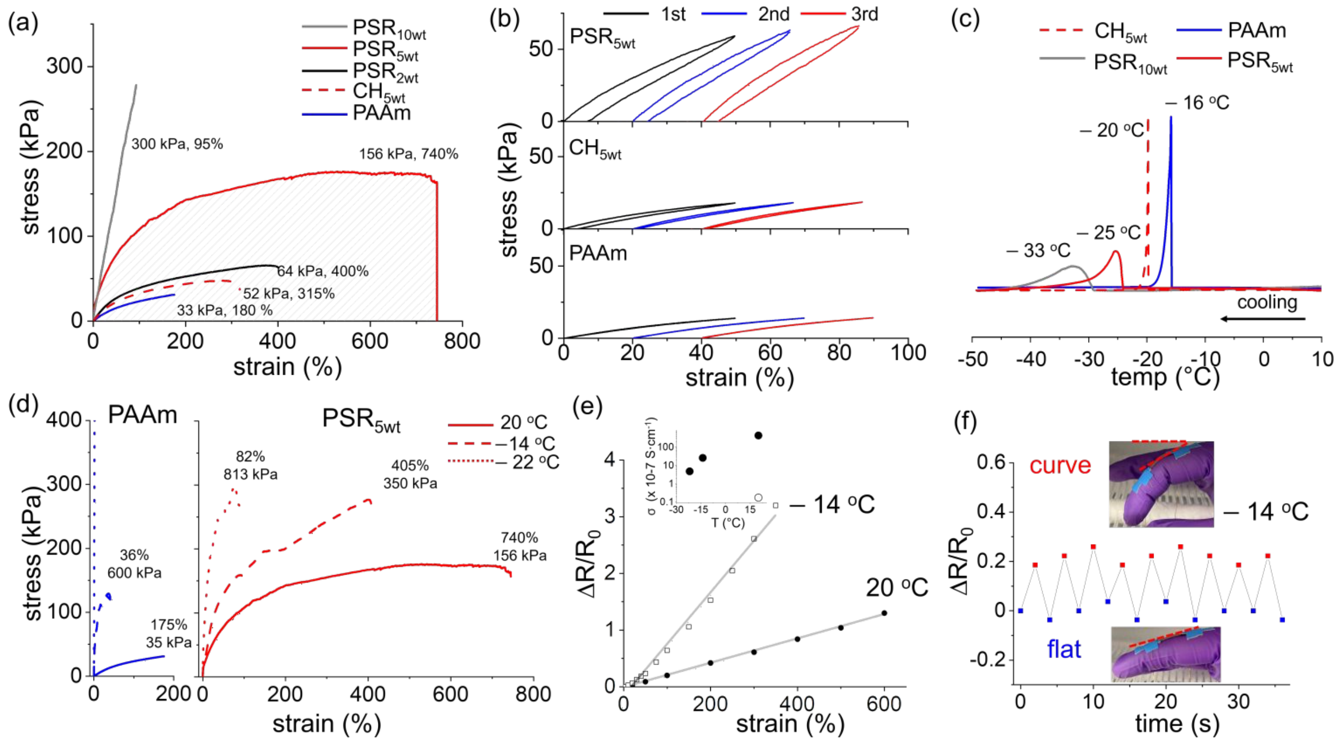

**Fig. 3** (a) Stress-strain measurements of the hydrogel samples. Each sample was stretched to rupture at a strain rate of 20 μm/s at 20°C. (b) Cyclic uniaxial stretch loading and unloading of hydrogel samples at a strain rate of 20 μm/s at 20°C. The hydrogels were each loaded to a strain of 50% below the value that would rupture the PAAm hydrogel, and then unloaded at 20°C. Each cycle was repeated 3 times and the second loading was applied immediately after the unloading in the former cycle. Horizontal shifts are applied to the 2nd and 3rd cycle curves for clarity. (c) DSC profiles of PAAm, $CH_{5wt}$, $PSR_{5wt}$, and $PSR_{10wt}$ hydrogels. Scanned from 10 °C to −50 °C at a rate of −5°C/min. (d) Stress-strain curves of PAAm, $PSR_{5wt}$ hydrogels at 20°C, −14°C and −22°C, respectively. Strain rate = 20 μm/s. (e) The resistance change ($\Delta R/R_0$) of $PSR_{5wt}$ hydrogel to applied uniaxial strain at 20 °C and −14 °C. Inset: The conductivity of $PSR_{5wt}$ (solid circle) at 20 °C, −14 °C and −22 °C and PAAm (empty circle) at 20 °C, respectively. (f) Cyclic resistance changes of a $PSR_{5wt}$ strain sensor as the finger (un)bent at −14 °C.

carboxymethylated CD rings to freely shuttle upon stretching, thereby dissipating energy. When the [Am]/[COOH] ratio is increased to 9:1, the α-CD-α-CD aggregations started to emerge (Fig. 2a), generating a rigid hydrogen-bonded network at the cost of limiting the mobility of carboxymethylated α-CDs in the crosslinked hydrogel.

To understand the contribution of the polyrotaxane in comparison to the mixture of its ring (carboxymethylated CD) and axle (adamantyl-capped $PEG_{35k}$, $PEG\text{-}Ad_2$) components, we synthesized a control hydrogel $CH_{5wt}$ using $PEG\text{-}Ad_2$ and carboxymethylated α-CD (4.7 carboxymethyl groups per α-CD molecule, Fig. S9). The $CH_{5wt}$ hydrogel possesses identical molecular entities as the $PSR_{5wt}$ hydrogel, but the carboxymethylated α-CDs could not thread onto the $PEG\text{-}Ad_2$ axle due to the presence of adamantyl bulky stoppers. The Young's modulus and strain at break of $CH_{5wt}$ hydrogel were measured to be 52 kPa and 315%, respectively (Fig. 3a), which is much less tough (33%) and stretchable (43%) relative to the $PSR_{5wt}$ hydrogel. These results highlight the benefit of the PSR network. The multivalent hydrogen-bonding interactions between $PR_{COOH}$ and PAAm increased the strength and toughness of the hydrogel. The carboxymethylated α-CD ring sliding motions and the exchange of the hydrogen-bonding site between the carboxylic acid groups of the α-CD and the amide groups of PAAm promote the network stretchability.

In cyclic (un)loading uniaxial stretch tests (Fig. 3b, *middle*), PAAm and $CH_{5wt}$ hydrogels exhibited negligible hysteresis at 50 % strain. In comparison, $PSR_{5wt}$ hydrogel showed pronounced hysteresis in these cyclic loading experiments (Fig. 3a, *top*). This result suggests that the restoration of the PSR network is slower than a traditional slide-ring hydrogel, since the PSR network is connected via multivalent hydrogen-bonding interactions, similar to hydrogen-bonded double networks.[35]

To explore the anti-freezing feature of these PSR hydrogels, differential scanning calorimetry (DSC, Fig. 3c) measurements were performed, and the freezing points of the PAAm[11] and $CH_{5wt}$ hydrogels are measured to be –16 °C and –20 °C, respectively. In comparison, the freezing points of $PSR_{5wt}$ and $PSR_{10wt}$ hydrogels decreased to –25 °C and –33 °C, accordingly (Fig. 3c). At the same scan rate in the DSC measurements, the exothermic profiles of $PSR_{5wt}$ and $PSR_{10wt}$ hydrogels are significantly broader than those of $CH_{5wt}$ and PAAm hydrogels, suggesting much slower ice formation kinetics in $PSR_{5wt}$ and $PSR_{10wt}$. Since $CH_{5wt}$ and $PSR_{5wt}$ hydrogels possess identical chemical components but different network architectures, the enhanced anti-freezing capability of $PSR_{5wt}$ hydrogel could be attributed to the PSR network. Compared to individual carboxymethylated α-CDs in the $CH_{5wt}$ hydrogel, the threaded carboxymethylated α-CDs in the PSR could trap more water molecules and prevent them from freezing.[36] When ice crystals are formed in the hydrogel, the carboxymethylated α-CD ring sliding motions enabled the dynamic adjustment of the local network, thus slowing down the propagation of the ice crystallization.

At sub-zero temperatures, the $PSR_{5wt}$ hydrogel remained stretchable (405 % of strain at –14 $^{o}$C, Fig. 3d) but the PAAm hydrogel became very brittle. At –22 $^{o}$C, the PAAm hydrogel was frozen (Fig. S23) but the $PSR_{5wt}$ hydrogel was stretched up to 182% before rupture. The $PSR_{5wt}$ hydrogel is ionically conductive at 20 $^{o}$C and –14 $^{o}$C (Fig. 3e, inset), which was attributed to the ionization of concentrated carboxylic groups in $PR_{COOH}$. The conductive feature of the $PSR_{5wt}$ hydrogel enabled us to fabricate a low-temperature strain sensor (40 × 8 × 2 mm, Fig. 3f inset). The change of resistance ($\Delta R/R_0$) of the hydrogel steadily increased when uniaxial strains were applied at both －4 $^{o}$C and 20 $^{o}$C before the sensor ruptures (Fig. 3e). The monitoring of motions was performed by attaching the hydrogel sensor onto a covered finger. The finger bending motions were operated at －14 $^{o}$C, and the $\Delta R/R_0$ of the sensor were recorded (Fig. 3f). Bending to 45$^{o}$ in 2 s, the resistance increased due to the extension of the hydrogel. The sensor exhibited reproducible resistance change without any significant signal decay after 9 bending/unbending cycles, demonstrating the durability of the PSR sensor.

In summary, we have developed a chemical approach to synthesize anti-freezing hydrogels with good mechanical properties through the introduction of a pseudo-slide-ring network. This network is comprised of carboxymethylated α-CD-threaded polyrotaxane and polyacrylamide polymers. The multivalent hydrogen-bonding interactions between the polyrotaxane and polyacrylamide increased the strength and toughness of the hydrogel. The ring-sliding motion and hydrogen-bonding site-exchange contributed to the enhanced stretchability. The ring sliding motion was discovered to retard the ice-crystallization. The formed $PSR_{5wt}$ hydrogel is stretchable and conductive at room temperature as well as －14 $^{o}$C, which enabled the fabrication of a cold-temperature strain sensor. Our work demonstrated an important example of enhancing macroscale properties through molecular design.

This work is supported by grants from the Beckman Young Investigator Program and Department of Energy the Basic Energy Sciences DE-SC0022267.

## Conflicts of interest

There are no conflicts to declare.

## Notes and references

1. M. A. English, L. R. Soenksen, R. V. Gayet, H. de Puig, N. M. Angenent-Mari, A. S. Mao, P. Q. Nguyen and J. J. Collins, *Science*, 2019, **365**, 780-785.
2. N. A. Peppas, J. Z. Hilt, A. Khademhosseini and R. Langer, *Adv. Mater.*, 2006, **18**, 1345-1360.
3. J. Y. Li and D. J. Mooney, *Nat. Rev. Mater.*, 2016, **1**, 1-17.
4. M. J. Webber and E. T. Pashuck, *Adv. Drug. Deliver. Rev.*, 2021, **172**, 275-295.
5. J. J. Green, J. H. Elisseeff, *Nature* 2016, **540**, 386–394.
6. I. R. Minev, P. Musienko, A. Hirsch, Q. Barraud, N. Wenger, E. M. Moraud, J. Gandar, M. Capogrosso, T. Milekovic, L. Asboth, R. F. Torres, N. Vachicouras, Q. H. Liu, N. Pavlova, S. Duis, A. Larmagnac, J. Voros, S. Micera, Z. G. Suo, G. Courtine and S. P. Lacour, *Science*, 2015, **347**, 159-163.
7. C. Lim, Y. J. Hong, J. Jung, Y. Shin, S. H. Sunwoo, S. Baik, O. K. Park, S. H. Choi, T. Hyeon, J. H. Kim, S. Lee and D. H. Kim, *Sci. Adv.*, 2021, **7**, eabd3716.
8. C. H. Yang and Z. G. Suo, *Nat. Rev. Mater.*, 2018, **3**, 125-142.
9. Y. Xu, Q. Rong, T. Zhao and M. Liu, *Giant*, 2020, **2**, 100014.
10. M. G. Potapczuk, *J. Aerospace. Eng.*, 2013, **26**, 260-276.
11. X. P. Morelle, W. R. Illeperuma, K. Tian, R. Bai, Z. Suo and J. J. Vlassak, *Adv. Mater.*, 2018, **30**, e1801541.
12. D. Lou, C. Wang, Z. He, X. Sun, J. Luo and J. Li, *Chem. Commun.*, 2019, **55**, 8422-8425.
13. Z. Liu, Y. Wang, Y. Ren, G. Jin, C. Zhang, W. Chen and F. Yan, *Mater. Horiz.*, 2020, **7**, 919-927.
14. Y. Jian, S. Handschuh-Wang, J. Zhang, W. Lu, X. Zhou and T. Chen, *Mater. Horiz.*, 2021, **8**, 351-369.
15. P. Wei, X. Yan, F. Huang, *Chem. Soc. Rev.* 2015, **44**, 815–832.
16. Z. He, C. Wu, M. Hua, S. Wu, D. Wu, X. Zhu, J. Wang and X. He, *Matter*, 2020, **2**, 723-734.
17. D. Zhang, Y. Liu, Y. Liu, Y. Peng, Y. Tang, L. Xiong, X. Gong and J. Zheng, *Adv. Mater.*, **2021**, 2104006.
18. K. G. Libbrecht, *Annu. Rev. Mater. Res.*, 2017, **47**, 271-295.
19. F. Mo, G. Liang, Q. Meng, Z. Liu, H. Li, J. Fan and C. Zhi, *Energy Envir. Sci.*, 2019, **12**, 706-715.
20. M. Osaki, S. Yonei, C. Ueda, R. Ikura, J. Park, H. Yamaguchi, A. Harada, M. Tanaka and Y. Takashima, *Macromolecules*, 2021, **54**, 8067–8076.
21. K. Mochizuki and V. Molinero, *J. Am. Chem. Soc.*, 2018, **140**, 4803-4811.
22. Y. C. Liou, A. Tocilj, P. L. Davies and Z. C. Jia, *Nature*, 2000, **406**, 322-324.
23. C. Stubbs, J. Lipecki and M. I. Gibson, *Biomacromolecules*, 2017, **18**, 295-302.
24. Y. Okumura and K. Ito, *Adv. Mater.*, 2001, **13**, 485-487.
25. C. Liu, N. Morimoto, L. Jiang, S. Kawahara, T. Noritomi, H. Yokoyama, K. Mayumi and K. Ito, *Science*, 2021, **372**, 1078-1081.
26. A. Bin Imran, K. Esaki, H. Gotoh, T. Seki, K. Ito, Y. Sakai and Y. Takeoka, *Nat. Commun.*, 2014, **5**, 5124.
27. C. Katsuno, A. Konda, K. Urayama, T. Takigawa, M. Kidowaki and K. Ito, *Adv. Mater.*, 2013, **25**, 4636-4640.
28. K. Mayumi, C. Liu, Y. Yasuda and K. Ito, *Gels*, 2021, **7**, 91.
29. M. Nakahata, S. Mori, Y. Takashima, H. Yamaguchi and A. Harada, *Chem*, 2016, **1**, 766-775.
30. H. Shirota and H. Ushiyama, *J. Phys. Chem. B*, 2008, **112**, 13542-13551.
31. Y. Yasuda, Y. Hidaka, K. Mayumi, T. Yamada, K. Fujimoto, S. Okazaki, H. Yokoyama and K. Ito, *J. Am. Chem. Soc.*, 2019, **141**, 9655-9663.
32. J. Araki and K. Ito, *J. Poly. Sci. A Poly. Chem.*, 2006, **44**, 6312-6323.
33. L. Y. Li, Q. M. Lin, M. Tang, E. H. R. Tsai and C. F. Ke, *Angew. Chem. Int. Ed.*, 2021, **60**, 10186-10193.
34. W.W. Graessley, *The Entanglement Concept in Polymer Rheology. Advances in Polymer Science*, Springer, Berlin, German, 1974.
35. Y. N. Ye, K. Cui, W. Hong, X. Li, C. Yu, D. Hourdet, T. Nakajima, T. Kurokawa and J. P. Gong, *Proc. Natl. Acad. Sci. U.S.A*, 2021, **118**, e2014694118.
36. Q. Lin, L. Li, M. Tang, S. Uenuma, J. Samanta, S. Li, X. Jiang, L. Zou, K. Ito and C. Ke, *Chem*, 2021, **7**, 2442–2459.